An a posteriori error estimator for hp-adaptive discontinuous Galerkin methods for computing band gaps in photonic crystals

S. Giani [*]

Abstract

In this paper we propose and analyze a hp-adaptive discontinuous finite element method for computing the band structure of 2D periodic photonic crystals. The problem can be reduced to the computation of the discrete spectrum of each member in a family of periodic Hermitian eigenvalue problems on the primitive cell, parametrised by a two-dimensional parameter - the quasimomentum. We propose a residual-based error estimator and show that it is reliable and efficient for all eigenvalue problems in the family. In particular we prove that if the error estimator converges to zero then the distance of the computed eigenfunction from the true eigenspace also converges to zero and the computed eigenvalue converges to a true eigenvalue. The results hold for eigenvalues of any multiplicity. We illustrate the benefits of the resulting hp-adaptive method in practice, both for fully periodic crystals and also for the computation of eigenvalues in the band gaps of crystals with defects.

1   Introduction

Photonic crystals (PCs) are constructed by assembling portions of periodic media composed of dielectric materials and they are designed to exhibit interesting properties in the propagation of electromagnetic waves, such as spectral band gaps - i.e., monochromatic electromagnetic waves of certain frequencies may not propagate inside them. Media with band gaps have

---
[*]School of Mathematical Sciences, University of Nottingham, University Park, Nottingham NG7 2RD, UK, email: `Stefano.Giani@nottingham.ac.uk`.

many potential applications, for example, in optical communications, filters, lasers, switches and optical transistors; see [22, 28, 23, 8] for an introduction. In this paper we consider only 2D PCs, whose structure is periodic in the plane determined by two orthogonal directions and is constant in the direction normal to that plane. The behavior of light in these kind of devices can be predicted solving a family of problems of the form: *seek eigenpairs of the form* $(\lambda, u) \in \mathbb{C} \times H^1_\pi(\Omega)$, *with u appropriately normalized, such that*

$$\int_\Omega (\mathcal{A}(\nabla + i\kappa)u) \cdot \overline{((\nabla + i\kappa)v)} \ = \ \lambda \int_\Omega \mathcal{B}u\overline{v} \quad \text{in } \Omega, \text{ for all } v \in H^1_\pi(\Omega), \quad (1.1)$$

where Ω is the primitive cell of the photonic crystal and $H^1_\pi(\Omega)$ is the space all functions of $H^1(\Omega)$ satisfying periodic boundary conditions on $\partial\Omega$. The scalar functions $\mathcal{A}$ and $\mathcal{B}$ in (1.1) are real and bounded above and below by positive constants for all $x \in \Omega$, i.e.

$$0 \ < \ \underline{a} \ \leq \ \mathcal{A}(x) \ \leq \ \overline{a} \quad \text{for all} \quad x \in \Omega, \quad (1.2)$$

$$0 \ < \ \underline{b} \ \leq \ \mathcal{B}(x) \ \leq \ \overline{b} \quad \text{for all} \quad x \in \Omega. \quad (1.3)$$

In this paper we will assume (as it is generally the case in applications), that $\mathcal{A}$ and $\mathcal{B}$ are both piecewise constant on Ω and we will also assume that any jumps in $\mathcal{A}$ and $\mathcal{B}$ are aligned with the meshes used in this work.

A very popular practical numerical method for PCs is the Fourier spectral method (also called the "plane-wave expansion method") [27, 22, 13, 25, 26]. This method exploits the periodicity in the PC and uses modern highly tuned FFT algorithms to obtain fast implementations. However the overall rate of convergence of approximate spectra to true spectra is slow because the jumps in the dielectric permittivity destroy the exponential accuracy which is achieved by Fourier spectral methods on smooth problems.

In recent years papers on finite element methods (FEMs) for PC problems have started to appear, especially on low order FEMs [10, 12, 14, 15]. Even more recently there has been considerable interest in h-adaptive and hp-adaptive FEMs. Examples of the former technology applied to PCs can be found in [21, 20]. In this paper we are going to focus in the latter technology which could achieve an exponential convergence rate. The are already examples of a priori hp-adaptive methods in [29, 30], but as far as we know a derivation for this problem of a reliable and efficient a posteriori error estimator with hp-adaptivity is still missing. Also in contrast to the majority of works mentioned above we are not using a continuous Galerkin method, but instead a discontinuous Galerkin (DG) method.

One of the main reasons why DG methods are widely used is because they offer advantages in the context of hp–adaptivity over standard conforming

FEMs. For example they provide increased flexibility in mesh design (irregular grids are admissible) and the freedom to choose the elemental polynomial degrees, without the need to enforce continuity between elements, make the realization of numerical codes simpler. It is already possible to find a DG method for PCs in [16]. However in that paper there is no a posteriori error analysis and also the DG method is different from the one presented here because it is non-Hermitian.

The paper is structured as follows. In the next section we derive the family of eigenvalue problems for photonic crystals. We then introduce the symmetric interior penalty discretisation for the model problem after first defining some appropriate function spaces and trace operators. The a posteriori error estimator is stated in Section 4 and its reliability and efficiency shown, up to higher order terms. In Section 5 we describe in details our numerical method and how we use it. Then we present two numerical experiments to validate our theoretical results. The first experiment is on periodic structure, while the second one is on a photonic crystal with a defect.

2 Photonic crystal eigenvalue problem

The mathematical development (see e.g. [23]) begins with the Maxwell's equations for a monochromatic electromagnetic wave of frequency ω:

$$\begin{array}{ll} \nabla \times \mathbf{E}_\omega = -\frac{i\omega}{c}\mu\mathbf{H}_\omega, & \nabla \cdot \mu\mathbf{H}_\omega = 0 \ , \\ \nabla \times \mathbf{H}_\omega = \frac{i\omega}{c}\varepsilon\mathbf{E}_\omega \ , & \nabla \cdot \varepsilon\mathbf{E}_\omega = 0 \ . \end{array} \tag{2.4}$$

where $\mathbf{E}_\omega$ is the electric field, $\mathbf{H}_\omega$ is the magnetic field, ε and μ are, respectively, the dielectric permittivity and magnetic permeability tensors, and c is the speed of light in a vacuum. We assume the medium is periodic in the (x, y) plane and is constant in the third (z) direction and that the material is non-magnetic (so $\mu = 1$). The problem (2.4) splits naturally into two independent problems, called transverse magnetic (TM) and transverse electric (TE) modes, as explained in [23]. On the assumption that the medium is isotropic (so ε is scalar-valued), the problems are

$$\Delta u_\omega + \frac{\omega^2}{c^2}\varepsilon u_\omega = 0 \quad \text{(TM case)} \ , \tag{2.5}$$

and

$$\nabla \cdot \frac{1}{\varepsilon}(\nabla u_\omega) + \frac{\omega^2}{c^2}u_\omega = 0, \quad \text{(TE case)} \ . \tag{2.6}$$

Both problems (2.5) and (2.6) may be written in the abstract form as that of seeking (λ, u) with $u \neq 0$ such that

$$\nabla \cdot (\mathcal{A}\nabla u) + \lambda\mathcal{B}u = 0 \ . \tag{2.7}$$

So far (2.7) is posed over $\mathbb{R}^2$, with periodic coefficients.

A 2D periodic medium can be described using a lattice $L := \{\mathbf{R} = n_1\mathbf{r}_1 + n_2\mathbf{r}_2 \ , \ n_1, n_2 \in \mathbb{Z}\}$, where $\{\mathbf{r}_1, \mathbf{r}_2\}$ is a basis for $\mathbb{R}^2$. The (Wigner-Seitz) primitive cell for L is the set Ω of all points in $\mathbb{R}^2$ which are closer to $\mathbf{0}$ than to any other point in L - see [9]. When $\overline{\Omega}$ is translated through all $\mathbf{R} \in L$, we obtain a covering of $\mathbb{R}^2$ with overlap of measure 0. The reciprocal lattice for L is the lattice $\hat{L}$ generated by a basis $\{\mathbf{k}_1, \mathbf{k}_2\}$, chosen so that $\mathbf{r}_i \cdot \mathbf{k}_j = 2\pi\delta_{i,j}$, $i, j = 1, 2$, where $\delta_{i,j}$ is the Kronecker delta and the primitive cell for the reciprocal lattice is called the *first Brillouin zone*, which we denote here by $\mathcal{K}$ [9].

For example, if L is the square lattice generated by $\{\mathbf{e}_1, \mathbf{e_2}\}$ (where $\mathbf{e}_i$ are the standard basis functions in $\mathbb{R}^2$), then $\Omega = [-0.5, 0.5]^2$, $\hat{L}$ is generated by $\{2\pi\mathbf{e}_1, 2\pi\mathbf{e_2}\}$ and the first Brillouin zone is $\mathcal{K} = [-\pi, +\pi]^2$. Such square lattices are used in all numerical experiments in Section 5.

The Floquet transform - see, e.g. [23] - may them be used to show the equivalence of the problem (2.7) to a family of problems on the primitive cell Ω parametrized by quasimomentum $\kappa \in \mathcal{K}$. This is the family

$$(\nabla + i\kappa) \cdot \mathcal{A}(\nabla + i\kappa)\tilde{u} + \lambda B\tilde{u} \ = \ 0 \quad \text{on } \Omega, \quad \kappa \in \mathcal{K} \ , \qquad (2.8)$$

where $\tilde{u}$ is the Floquet transform of u and λ is the corresponding eigenvalue which now depends on κ. This equation should again be understood in the weak form - a rigorous derivation can be found for example in [11]. In order to recover the spectrum of the problem (2.7), it is sufficient to compute the union of all the spectra of the problems in the family (2.8) for all $\kappa \in \mathcal{K}$, and these problems have discrete spectra [23]. Writing (2.8) in weak form gives precisely (1.1).

Throughout $L^2(\Omega)$ denotes the usual space of square integrable complex valued functions equipped with the weighted norm

$$\|f\|_{0,\mathcal{B}} \ = \ b(f, f)^{1/2} \ , \quad b(f, g) := \int_\Omega \mathcal{B}f\bar{g} \ . \qquad (2.9)$$

$H^1(\Omega)$ denotes the usual space of functions in $L^2(\Omega)$ with square integrable gradient, with H^1-norm denoted $\|f\|_1$, and $H^1_\pi(\Omega)$ denotes the subspace of functions in $f \in H^1(\Omega)$ which satisfy periodic boundary conditions on $\partial\Omega$. We will also need the fractional order spaces $H^{1+s}(\Omega)$, $s \in [0, 1]$. When we want to restrict these norms to a measurable subset $S \subseteq \Omega$, we write $\|f\|_{0,\mathcal{B},S}$, $\|f\|_{1,S}$, etc.

Problem (1.1) can be rewritten as: *seek eigenpairs of the form* $(\lambda_j, u_j) \in \mathbb{R} \times H^1_\pi(\Omega)$ *such that*

$$\left. \begin{array}{rcll} a_\kappa(u_j, v) & = & \lambda_j \, b(u_j, v) \ , & \text{for all} \quad v \in H^1_\pi(\Omega) \\ \|u_j\|_{0,\mathcal{B}} & = & 1 \ , & \end{array} \right\} \qquad (2.10)$$

where

$$a_\kappa(u,v) := \int_\Omega (\mathcal{A}(\nabla + i\kappa)u) \cdot \overline{((\nabla + i\kappa)v)} \ , \quad b(u,v) := \int_\Omega \mathcal{B}u\overline{v} \ .$$

It is easy to see that a_κ is a Hermitian form on $H^1_\pi(\Omega)$, which is bounded on $H^1(\Omega)$ independently of $\kappa \in \mathcal{K}$.

3   Discontinuous Galerkin discretization

In this section, we introduce the hp-version of the symmetric interior penalty (SIP) finite element method for the discretization of (2.10). Our formulation differs from the formulation in [16] because it is Hermitian and due to the design of the penalty parameter, it is suitable for hp-adaptivity.

Throughout, we assume that the computational domain Ω can be partitioned into a shape-regular triangulation $\mathcal{T}$, i.e. there exists a constant C_{reg} such that for any element K

$$h_K \leq C_{\mathrm{reg}} \ \rho_K \ , \tag{3.11}$$

where h_K is the diameter of the element and ρ_K is the diameter of the biggest ball inscribed in K. Also we assume that the elements are affine triangles. We store the elemental diameters in the mesh size vector $\underline{h} = \{ h_K : K \in \mathcal{T} \}$. Let us also denote by h the maximum of all h_K in the mesh. We refer to F as an interior mesh face of $\mathcal{T}$ if $F = \partial K \cap \partial K'$ for two neighboring elements $K, K' \in \mathcal{T}$ whose intersection has a positive surface measure. For PC problems we do not have any boundary faces because problem (2.10) is subject to periodic boundary conditions, therefore all faces of the mesh along $\partial\Omega$ are actually interior faces, too. For this reason we don't need to treat the faces on $\partial\Omega$ differently from any other face in the interior of the mesh. The set of all interior mesh faces is denoted by $\mathcal{F}(\mathcal{T})$, the diameter of a face F is denoted by h_F. We allow for 1-irregularly refined meshes $\mathcal{T}$ defined as follows. Let K be an element of $\mathcal{T}$ and F an elemental face in $\mathcal{F}(K)$, then F may contain at most one hanging node located in the center of F and at most one hanging node in the middle of each elemental face of F.

In order to define the hp-version finite element space on $\mathcal{T}$, we begin by introducing polynomial spaces on elements and faces. To that end, let $K \in \mathcal{T}$ be an element, we set $\mathcal{P}_p(K)$ to be the set of polynomials on the element K of total degree less than or equal to p. Similarly for any face $F \in \mathcal{F}(K)$ we define $\mathcal{P}_p(F)$ to be he set of polynomials on F of total degree less than or equal to p. Then, we assign a polynomial degree $p_K \geq 1$ with each element K of the mesh $\mathcal{T}$. We then introduce the degree vector $\underline{p} = \{ p_K : K \in \mathcal{T} \}$.

We assume that $\underline{p}$ is of bounded local variation, that is, there is a constant $\varrho \geq 1$, independent of the mesh $\mathcal{T}$ sequence under consideration, such that

$$\varrho^{-1} \leq p_K/p_{K'} \leq \varrho \qquad (3.12)$$

for any pair of neighboring elements $K, K' \in \mathcal{T}$. For a mesh face $F \in \mathcal{F}(\mathcal{T})$, we introduce the face polynomial degree p_F by

$$p_F = \max\{p_K, p_{K^e}\}, \qquad \text{if } F = \partial K \cap \partial K^e \in \mathcal{F}(\mathcal{T}). \qquad (3.13)$$

Let us also denote by p the minimum of all p_K in the mesh.

For a partition $\mathcal{T}$ of Ω and a polynomial degree vector $\underline{p}$ on $\mathcal{T}$, we define the hp-version DG finite element spaces by

$$S_{\underline{p}}(\mathcal{T}) = \{\, v \in L^2(\Omega) \,:\, v|_K \in \mathcal{P}_{p_K}(K), \ K \in \mathcal{T} \,\}. \qquad (3.14)$$

$$\Sigma_{\underline{p}}(\mathcal{T}) = \{\, v \in [L^2(\Omega)]^2 \,:\, v|_K \in [\mathcal{P}_{p_K}(K)]^2, \ K \in \mathcal{T} \,\}. \qquad (3.15)$$

Next, we define some trace operators that are required for the DG methods. Let K^+ and K^- be two adjacent elements of $\mathcal{T}$, and $F \in \mathcal{F}(\mathcal{T})$ given by $F = \partial K^+ \cap \partial K^-$. Furthermore, let v be a complex scalar-valued function and let τ be a complex vector-valued function, that are smooth inside each element $K^\pm$. By $v^\pm$ and $\tau^\pm$, we denote the traces of v and τ on $\mathcal{F}$ taken from within the interior of $K^\pm$, respectively. Then, since we are dealing with jumping coefficients we need to use the definition of the weighted average of the diffusive flux $\mathcal{A}\tau$, for any $\tau \in \Sigma_{\underline{p}}(\mathcal{T})$, along $F \in \mathcal{F}(\mathcal{T})$ introduced in [34]

$$\{\!\{\mathcal{A}\tau\}\!\} = \omega^-(\mathcal{A}\tau)^- + \omega^+(\mathcal{A}\tau)^+ \,,$$

where

$$\omega^- = \frac{\mathbf{n}_{K^+}^t \mathcal{A}^+ \mathbf{n}_{K^+}}{\mathbf{n}_{K^-}^t \mathcal{A}^- \mathbf{n}_{K^-} + \mathbf{n}_{K^+}^t \mathcal{A}^+ \mathbf{n}_{K^+}} \,, \qquad \omega^+ = \frac{\mathbf{n}_{K^-}^t \mathcal{A}^- \mathbf{n}_{K^-}}{\mathbf{n}_{K^-}^t \mathcal{A}^- \mathbf{n}_{K^-} + \mathbf{n}_{K^+}^t \mathcal{A}^+ \mathbf{n}_{K^+}} \,,$$

where we denote by $\mathbf{n}_{K^\pm}$ the unit outward normal vector of $\partial K^\pm$, respectively. Similarly, for a scalar function $v \in S_{\underline{p}}(\mathcal{T})$ we have the following weighted average

$$\{\!\{v\}\!\} = \omega^- v^+ + \omega^+ v^- \,.$$

Then, the jump of v and τ across $F \in \mathcal{F}(\mathcal{T})$ is given by

$$[\![v]\!] = v^+ \, \mathbf{n}_{K^+} + v^- \, \mathbf{n}_{K^-}, \quad [\![\mathcal{A}\tau]\!] = (\mathcal{A}\tau)^+ \cdot \mathbf{n}_{K^+} + (\mathcal{A}\tau)^- \cdot \mathbf{n}_{K^-}.$$

The derivation of the SIP method for the operator in (2.10) follows the argument in [1]. First we write the problem $-(\nabla + i\kappa) \cdot (\mathcal{A}(\nabla + i\kappa)u) = f\mathcal{B}$, for all f in $L^2(\Omega)$, as a first order system with periodic boundary conditions:

$$\sigma = \mathcal{A}(\nabla + i\kappa)u, \quad -(\nabla + i\kappa) \cdot \sigma = f\mathcal{B} \quad \text{in } \Omega, \qquad (3.16)$$

which should be intended in weak form. Then we consider the following general discrete problem of the variational formulation of (3.16): Find $u_{hp} \in S_{\underline{p}}(\mathcal{T})$ such that for all $K \in \mathcal{T}$ we have

$$\int_K \sigma_{hp} \cdot \overline{\tau}\,dx \;=\; -\int_K u_{hp}\overline{(\nabla + i\kappa)} \cdot (\mathcal{A}\overline{\tau})\,dx$$
$$+ \int_{\partial K} \widehat{u}_K\, \mathcal{A}_K \overline{\tau} \cdot \underline{n}_K\,ds \quad \forall \tau \in \Sigma_{\underline{p}}(\mathcal{T})\;,\;(3.17)$$
$$\int_K \sigma_{hp} \cdot \overline{(\nabla + i\kappa)v}\,dx \;=\; \int_K \mathcal{B}f\,\overline{v}\,dx$$
$$+ \int_{\partial K} \widehat{\sigma}_K \cdot \underline{n}_K\overline{v}\,ds \quad \forall v \in S_{\underline{p}}(\mathcal{T})\;,\qquad(3.18)$$

where the numerical fluxes $\widehat{u} = (\widehat{u}_K)_{K \in \mathcal{T}}$ and $\widehat{\sigma} = (\widehat{\sigma}_K)_{K \in \mathcal{T}}$ are approximations of u and σ, which are defined as

$$\widehat{u} : H^1(\mathcal{T}) \to T(\Gamma), \quad \widehat{\sigma} : H^2(\mathcal{T}) \times [H^1(\mathcal{T})]^2 \to [T(\Gamma)]^2\;,$$

where the space $H^s(\mathcal{T}) \subset L^2(\Omega)$ contains all the functions whose restriction to each element K belongs to $H^s(K)$ and where $T(\Gamma) := \Pi_{K \in \mathcal{T}}L^2(\partial K)$. Summing (3.17) and (3.18) over all elements K we obtain

$$\int_\Omega \sigma_{hp} \cdot \overline{\tau}\,dx = -\int_\Omega u_{hp}\overline{(\nabla + i\kappa)} \cdot (\mathcal{A}\overline{\tau})\,dx + \sum_{K \in \mathcal{T}} \int_{\partial K} \widehat{u}_K\, \mathcal{A}_K \overline{\tau} \cdot \underline{n}_K\,ds\;,$$
$$\int_\Omega \sigma_{hp} \cdot \overline{(\nabla + i\kappa)v}\,dx = \int_\Omega \mathcal{B}f\,\overline{v}\,dx + \sum_{K \in \mathcal{T}} \int_{\partial K} \widehat{\sigma}_K \cdot \underline{n}_K\overline{v}\,ds\;,$$

and then using the identity

$$\sum_{K \in \mathcal{T}} \int_{\partial K} q_K \mathcal{A}_K \overline{\phi}_K \cdot \underline{n}_K\,ds = \int_\Gamma [\![q]\!] \cdot \{\!\{\mathcal{A}\overline{\phi}\}\!\} + \{\!\{q\}\!\}[\![\mathcal{A}\overline{\phi}]\!]\,ds\;,$$

we obtain taking $v = u_{hp}$

$$\int_\Omega \sigma_{hp} \cdot \overline{\tau}\,dx \;=\; -\int_\Omega u_{hp}\overline{(\nabla + i\kappa)} \cdot (\mathcal{A}\overline{\tau})\,dx$$
$$+ \int_\Gamma [\![\widehat{u}]\!] \cdot \{\!\{\mathcal{A}\overline{\tau}\}\!\} + \{\!\{\widehat{u}\}\!\}[\![\mathcal{A}\overline{\tau}]\!]\,ds \qquad(3.19)$$
$$\int_\Omega \sigma_{hp} \cdot \overline{(\nabla + i\kappa)v}\,dx \;=\; \int_\Omega \mathcal{B}f\,\overline{v}\,dx + \int_\Gamma [\![\overline{v}]\!] \cdot \{\!\{\widehat{\sigma}\}\!\} + \{\!\{\overline{v}\}\!\}[\![\widehat{\sigma}]\!]\,ds\;(3.20)$$

Using the following identity on (3.19)

$$-\int_\Omega v\overline{(\nabla + i\kappa)} \cdot (\mathcal{A}\overline{\tau})\,dx = \int_\Omega \mathcal{A}(\nabla + i\kappa)v \cdot \overline{\tau}\,dx - \int_\Gamma [\![v]\!] \cdot \{\!\{\mathcal{A}\overline{\tau}\}\!\} + \{\!\{v\}\!\}[\![\mathcal{A}\overline{\tau}]\!]\,ds\;,$$

we obtain

$$\int_\Omega \sigma_{hp} \cdot \overline{\tau}\,dx = \int_\Omega \mathcal{A}(\nabla + i\kappa)u_{hp} \cdot \overline{\tau}\,dx + \int_\Gamma [\![\widehat{u} - u_{hp}]\!] \cdot \{\!\{\mathcal{A}\overline{\tau}\}\!\} + \{\!\{\widehat{u} - u_{hp}\}\!\}[\![\mathcal{A}\overline{\tau}]\!]\,ds\ .$$
(3.21)

Recalling that $(\nabla + i\kappa)S_{\underline{p}}(\mathcal{T}) \subset \Sigma_{\underline{p}}(\mathcal{T})$ and defining the lifting operators: $r : [L^2(\Gamma)]^2 \to \Sigma_{\underline{p}}(\mathcal{T})$ and $\overline{l} : L^2(\Gamma) \to \Sigma_{\underline{p}}(\mathcal{T})$ by

$$\int_\Omega r(\varphi) \cdot \mathcal{A}\overline{\tau}\,dx = -\int_\Gamma \varphi \cdot \{\!\{\mathcal{A}\overline{\tau}\}\!\}\,ds\ ,\quad \int_\Omega l(q) \cdot \mathcal{A}\overline{\tau}\,dx = -\int_\Gamma q[\![\mathcal{A}\overline{\tau}]\!]\,ds\ ,$$

we may rewrite (3.21) as

$$\sigma_{hp} := \mathcal{A}(\nabla + i\kappa)u_{hp} - \mathcal{A}\,r([\![\widehat{u} - u_{hp}]\!]) - \mathcal{A}\,l(\{\!\{\widehat{u} - u_{hp}\}\!\}) \tag{3.22}$$

Then substituting (3.22) in (3.20) we obtain

$$\int_\Omega \mathcal{A}(\nabla + i\kappa)u_{hp} \cdot \overline{(\nabla + i\kappa)v}\,dx + \int_\Gamma [\![\widehat{u} - u_{hp}]\!] \cdot \{\!\{\mathcal{A}\overline{(\nabla + i\kappa)v}\}\!\}\,ds$$

$$+ \int_\Gamma \{\!\{\widehat{u} - u_{hp}\}\!\}[\![\mathcal{A}\overline{(\nabla + i\kappa)v}]\!] - \{\!\{\widehat{\sigma}\}\!\} \cdot [\![\overline{v}]\!] - [\![\widehat{\sigma}]\!]\{\!\{\overline{v}\}\!\}\,ds$$

$$= \int_\Omega \mathcal{B}f\overline{v}\,dx\ . \tag{3.23}$$

Finally defining the numerical fluxes as $\widehat{u} := \{\!\{Iu_{hp}\}\!\}$ and $\widehat{\sigma} := \{\!\{\mathcal{A}(\nabla + i\kappa)u_{hp}\}\!\} - \gamma p_F^2/h_F[\![u_{hp}]\!]$ and choosing $f = \lambda_{hp}u_{hp}$ we obtain the SIP method of (2.10): Find $(\lambda_{hp}, u_{hp}) \in \mathbb{R} \times S_{\underline{p}}(\mathcal{T})$ such that

$$a_{hp,\kappa}(u_{hp}, v_{hp}) = \lambda_{hp}\,b(u_{hp}, v_{hp}) \qquad \forall\,v_{hp} \in S_{\underline{p}}(\mathcal{T}), \tag{3.24}$$

and with $\|u_{hp}\|_0 = 1$, where

$$a_{hp,\kappa}(u, v) = \sum_{K \in \mathcal{T}} \int_K \mathcal{A}(\nabla + i\kappa)u \cdot \overline{(\nabla + i\kappa)v}\,dx$$

$$- \sum_{F \in \mathcal{F}(\mathcal{T})} \int_F \left(\{\!\{\mathcal{A}(\nabla + i\kappa)u\}\!\} \cdot [\![\overline{v}]\!] + \{\!\{\mathcal{A}\overline{(\nabla + i\kappa)v}\}\!\} \cdot [\![u]\!]\right)ds$$

$$+ \sum_{F \in \mathcal{F}(\mathcal{T})} \frac{\gamma p_F^2}{h_F} \int_F [\![u]\!] \cdot [\![\overline{v}]\!]\,ds\ ,$$
(3.25)

where the parameter $\gamma > 0$ is the interior penalty parameter.

We need another norm in the analysis, the following norm is the modification for PC problems of the DG norm already used in [6, 35]:

Definition 3.1 (Energy norm): For any $u \in \mathcal{S}(h) := S_{\underline{p}}(\mathcal{T}) + H^1(\Omega)$

$$\| u \|^2_{\mathrm{E},\mathcal{T}} = \sum_{K \in \mathcal{T}} \|u\|^2_{1,K} + \sum_{F \in \mathcal{F}(\mathcal{T})} \frac{\gamma p_F^2}{h_F} \|[\![u]\!]\|^2_{0,F}. \tag{3.26}$$

To be able to carry on the a posteriori analysis, we must perform a non-consistent reformulation of the DG discretization (3.24). To this end, we introduce the following lifting operator already used in [5, 1]. For any v belonging to $\mathcal{S}(h)$, we define $\mathcal{L}(v) \in \Sigma_{\underline{p}}(\mathcal{T})$ by $\mathcal{L}(v) := -r([\![v]\!])$. Now the following extended bilinear form $\tilde{a}_{hp,\kappa}(u,v)$ can be introduced:

$$\tilde{a}_{hp,\kappa}(u,v) = \sum_{K \in \mathcal{T}} \int_K \mathcal{A}(\nabla + i\kappa)u \cdot \overline{(\nabla + i\kappa)v}\, dx$$

$$- \sum_{K \in \mathcal{T}} \int_K \mathcal{A}\mathcal{L}(u) \cdot \overline{(\nabla + i\kappa)v} + \mathcal{A}\mathcal{L}(\overline{v}) \cdot (\nabla + i\kappa)u\, dx \tag{3.27}$$

$$+ \sum_{F \in \mathcal{F}(\mathcal{T})} \frac{\gamma p_F^2}{h_F} \int_F [\![u]\!] \cdot [\![\overline{v}]\!]\, ds = \lambda \int_\Omega u\mathcal{B}\overline{v}\, dx .$$

Remark 3.2: It is clear that $\tilde{a}_{hp,\kappa}(\cdot,\cdot) \equiv a_{hp,\kappa}(\cdot,\cdot)$ on $S_{\underline{p}}(\mathcal{T}) \times S_{\underline{p}}(\mathcal{T})$ and $\tilde{a}_{hp,\kappa}(\cdot,\cdot) \equiv a(\cdot,\cdot)$ on $H^1_\pi(\Omega) \times H^1_\pi(\Omega)$.

It is easy to see that both $a_{hp,\kappa}$ and $\tilde{a}_{hp,\kappa}$ are Hermitian forms and by the positiveness of $\mathcal{A}$ assumed in (1.2), we have

$$\tilde{a}_{hp,\kappa}(u,u) \geq \underline{a} \int_\Omega |(\nabla + i\kappa)u|^2 \geq 0 , \quad \text{for all } u \in H^1_\pi(\Omega) . \tag{3.28}$$

Since $\tilde{a}_{hp,\kappa}(u,u)$ is not always strictly positive (for $u \neq 0$), since if $\kappa = (0,0)$ then $\tilde{a}_{hp,\kappa}(1,1) = 0$. Thus we introduce the shifted Hermitian form: $\tilde{a}_{hp,\kappa,s}(u,v) := \tilde{a}_{hp,\kappa}(u,v) + s\, b(u,v)$ with the fixed shift $s := \max_{\kappa \in \mathcal{K}} |\kappa|^2 \underline{a}/\underline{b} + 1$. Similarly we introduce also the shifted Hermitian form $a_{hp,\kappa,s}(u,v) := a_{hp,\kappa}(u,v) + s\, b(u,v)$. These shifted forms are never used in the computations, only in the analysis.

So the shifted versions of problems (2.10), (3.24), (3.27) are: *Seek eigenpairs of the form $(\delta_j, u_j) \in \mathbb{R} \times H^1_\pi(\Omega)$ such that*

$$\left. \begin{array}{rll} a_{\kappa,s}(u_j,v) &=& \delta_j\, b(u_j,v) , \quad \text{for all} \quad v \in H^1_\pi(\Omega) \\ \|u_j\|_{0,\mathcal{B}} &=& 1 \end{array} \right\} \tag{3.29}$$

Seek eigenpairs of the form $(\delta_{j,hp}, u_{j,hp}) \in \mathbb{R} \times S_{\underline{p}}(\mathcal{T})$ such that

$$\left. \begin{array}{rll} a_{hp,\kappa,s}(u_{j,hp},v_{hp}) &=& \delta_{j,hp}\, b(u_{j,hp},v_{hp}) \quad \forall\, v_{hp} \in S_{\underline{p}}(\mathcal{T}), \\ \|u_{j,hp}\|_{0,\mathcal{B}} &=& 1 \end{array} \right\} \tag{3.30}$$

Seek eigenpairs of the form $(\delta_j, u_j) \in \mathbb{R} \times \mathcal{S}(h)$ *such that*

$$
\left.
\begin{array}{rll}
\tilde{a}_{hp,\kappa,s}(u_j, v) & = & \delta_j \, b(u_j, v) \,, \quad \text{for all} \quad v \in \mathcal{S}(h) \\
\|u_j\|_{0,\mathcal{B}} & = & 1
\end{array}
\right\}
\qquad (3.31)
$$

The presence of the value s shifts the spectrum by a length s, keeping the eigenfunctions the same. So for example if $(\lambda_{j,hp}, u_{j,hp})$ is an eigenpair of (3.24), then $(\delta_{j,hp}, u_{j,hp})$ is an eigenpair of (3.30) with $\lambda_{j,hp} = \delta_{j,hp} - s$.

It is possible to prove, reworking the proofs in [5, Lemma 4.3, Lemma 4.4], that the bilinear form $\tilde{a}_{hp,\kappa,s}(\cdot,\cdot)$ is continuous on $\mathcal{S}(h)$, i.e.,

$$
|\tilde{a}_{hp,\kappa,s}(u,v)| \leq C_{\tilde{\mathcal{A}}} \| u \|_{\mathrm{E},\mathcal{T}} \, \| v \|_{\mathrm{E},\mathcal{T}} \,, \qquad (3.32)
$$

with a constant $C_{\tilde{\mathcal{A}}} > 0$ independent of h and p, and that it is also coercive in $H^1_p i(\Omega)$, i.e.,

$$
\| u \|^2_{\mathrm{E},\mathcal{T}} \lesssim \tilde{a}_{hp,\kappa,s}(u,u) \,.
$$

The distance of an approximate eigenfunction from the true eigenspace is a crucial quantity in the convergence analysis for eigenvalue problems especially in the case of non-simple eigenvalues.

Definition 3.3: Given a function $v \in L^2(\Omega)$ and a finite dimensional subspace $\mathcal{P} \subset L^2(\Omega)$, we define:

$$
\mathrm{dist}(v, \mathcal{P})_0 \ := \ \min_{w \in \mathcal{P}} \| v - w \|_0 \,. \qquad (3.33)
$$

Similarly, given a function $v \in S_{\underline{p}}(\mathcal{T})$ and a finite dimensional subspace $\mathcal{P} \subset H^1_\pi(\Omega)$, we define:

$$
\mathrm{dist}(v, \mathcal{P})_{\mathrm{E},\mathcal{T}} \ := \ \min_{w \in \mathcal{P}} \| v - w \|_{\mathrm{E},\mathcal{T}} \,. \qquad (3.34)
$$

Lemma 3.5 links together the two quantities of interest in the convergence analysis, namely the error in the eigenvalues and the error in the eigenfunctions.

Definition 3.4 (Residual of the eigenvalue problem): Let define the residual of (3.31)

$$
\mathcal{R}(u_j, v) \ := \ \tilde{a}_{hp,\kappa,s}(u_j, v) - \delta_j b(u_j, v) \,, \qquad (3.35)
$$

where $u \in H^s(\Omega)$, with $s \geq 2$, is the solution of the linear problem and $v \in \mathcal{S}(h)$.

Lemma 3.5 (Identity result for the extended form): Let (λ_l, u_l) be a true eigenpair of problem (2.10) with $\|u_l\|_0 = 1$ and let $(\lambda_{j,hp}, u_{j,hp})$ be a computed eigenpair of problem (3.24) with $\|u_{j,hp}\|_0 = 1$. Then we have:

$$\tilde{a}_{hp,\kappa,s}(u_l - u_{j,hp}, u_l - u_{j,hp}) \;=\; \delta_l \|u_l - u_{j,hp}\|_0^2 \;+\; \delta_{j,hp} - \delta_l + 2\mathcal{R}(u_l, u_j - u_{j,hp}).$$

Proof. Using the linearity of the bilinear form $\tilde{a}_{hp,\kappa}(\cdot, \cdot)$ and using (3.29) , (3.24); we have

$$\tilde{a}_{hp,\kappa,s}(u_l - u_{j,hp}, u_l - u_{j,hp}) \;=\; \delta_l + \delta_{j,hp} - 2\tilde{a}_{hp,\kappa,s}(u_l, u_{j,hp}) + 2\delta_l b(u_l, u_{j,hp}) - 2\delta_l b(u_l, u_{j,hp}) \,. \tag{3.36}$$

Furthermore, by analogous arguments we obtain

$$\|u_l - u_{j,hp}\|_0^2 \;=\; 2 \;-\; 2b(u_l, u_{j,hp}). \tag{3.37}$$

Substituting (3.37) into (3.36) we obtain

$$\tilde{a}_{hp,\kappa,s}(u_l - u_{j,hp}, u_l - u_{j,hp}) \;=\; \delta_l \|u_l - u_{j,hp}\|_0^2 + \delta_{j,hp} - \delta_l - 2\tilde{a}_{hp,\kappa,s}(u_l, u_{j,hp}) + 2\delta_l b(u_l, u_{j,hp}) \,.$$

Finally noticing that $\tilde{a}_{hp,\kappa,s}(u_l, u_j) = \delta_l b(u_l, u_j)$ and using (3.35) we obtain the result. ∎

Remark 3.6: Since problems (3.30), (3.31) are Hermitian, all the missing proofs of continuity and coercivity for the the bilinear forms and consequently the proof of a priori convergence for such problems can be reworked form the proofs in [33].

4   Residual-based error estimator

In this section we write $A \lesssim B$ when A/B is bounded by a constant which may depend on the functions $\mathcal{A}$ in (1.2) and $\mathcal{B}$ in (1.3), on $\underline{a}$, $\overline{a}$, $\underline{b}$ and $\overline{b}$, on C_{reg} in (3.11), ϱ in (3.12), γ in (3.25), the size of $\mathcal{K}$ and on the shift s. The hidden constant never depends on h or p.

Let $(\lambda_{j,hp}, u_{j,hp})$ be a computed eigenpair of (3.24). For each element $K \in \mathcal{T}$, we introduce the following local error indicator $\eta_{j,K}$ which is given by the sum of the three terms:

$$\eta_{j,K}^2 = \eta_{j,R_K}^2 + \eta_{j,F_K}^2 + \eta_{j,J_K}^2 \,, \tag{4.38}$$

where the first term η_{j,R_K} is the residual in the interior of the element K:

$$\eta_{j,R_K}^2 = p_K^{-2} h_K^2 \|\lambda_{j,hp} \mathcal{B} u_{j,hp} + (\nabla + i\kappa) \cdot \mathcal{A}(\nabla + i\kappa) u_{j,hp}\|_{0,K}^2 \,,$$

the second term η_{j,F_K} is the residual on the faces of K:

$$\eta_{j,F_K}^2 = \frac{1}{2} \sum_{F \in \mathcal{F}(K)} p_F^{-1} h_F \|[\![\mathcal{A}(\nabla + i\kappa)u_{j,hp}]\!]\|_{0,F}^2 ,$$

and finally the residual η_{j,J_K} measures the jumps on the faces of K of the approximate solution $u_{j,hp}$:

$$\eta_{j,J_K}^2 = \frac{1}{2} \sum_{F \in \mathcal{F}(K)} \frac{\gamma^2 p_F^3}{h_F} \|[\![u_{j,hp}]\!]\|_{0,F}^2.$$

Summing (4.38) on all elements we obtain the global error estimator η_j:

$$\eta_j^2 = \sum_{K \in \mathcal{T}} \eta_{j,K}^2. \tag{4.39}$$

Remark 4.1: In the definition of residual-based error estimators in other works, e.g. [33], the faces on the boundary of the domain Ω and the faces in the interior contribute differently to the error estimator. Instead, in (4.39) all faces contribute in the same way due to the periodic boundary condition imposed on $\partial\Omega$.

We recall the standard hp-approximation results from [3, Lemma 3.7]: For any $v \in H^1_\pi(\Omega)$, there exists a function $v_{hp} \in S_{\underline{p}}(\mathcal{T})$ such that

$$p_K^2 h_K^{-2} \|v - v_{hp}\|_{0,K}^2 \lesssim \|\nabla v\|_{0,K}^2,$$
$$\|\nabla(v - v_{hp})\|_{0,K}^2 \lesssim \|\nabla v\|_{0,K}^2, \tag{4.40}$$
$$p_K h_K^{-1} \|v - v_{hp}\|_{0,\partial K}^2 \lesssim \|\nabla v\|_{0,K}^2,$$

for any element $K \in \mathcal{T}$.

In order to prove the reliability, we decompose a computed eigenfunction $u_{j,hp}$ into a conforming part and a remainder:

$$u_{j,hp} = u_{j,hp}^c + u_{j,hp}^r,$$

where $u_{j,hp}^c = I_{hp}u_{j,hp} \in S_{\underline{p}}^c(\mathcal{T}) \subset H^1_\pi(\Omega)$ is defined using the averaging operator I_{hp} in [5, Lemma 4.6] for which the following results holds:

$$\sum_{K \in \mathcal{T}} \|\nabla(v - I_{hp}v)\|_{0,K}^2 \lesssim \sum_{F \in \mathcal{F}(\mathcal{T})} p_F^2 h_F^{-1} \|[\![v]\!]\|_{0,F}^2, \tag{4.41}$$

$$\sum_{K \in \mathcal{T}} \|v - I_{hp}v\|_{0,K}^2 \lesssim \sum_{F \in \mathcal{F}(\mathcal{T})} p_F^{-2} h_F \|[\![v]\!]\|_{0,F}^2. \tag{4.42}$$

Then the remainder $u^r_{j,hp}$ is given by $u^r_{j,hp} = u_{j,hp} - u^c_{j,hp} \in S_{\underline{p}}(\mathcal{T})$.

$$\| u_j - u_{j,hp} \|_{\mathrm{E},\mathcal{T}} \leq \| u_j - u^c_{j,hp} \|_{\mathrm{E},\mathcal{T}} + \| u^r_{j,hp} \|_{\mathrm{E},\mathcal{T}} . \tag{4.43}$$

Then to prove reliability for eigenfunctions it is just necessary to bound both terms in the right hand side of (4.43) using η_j. The proof that

$$\| u^r_{hp} \|_{\mathrm{E},\mathcal{T}} \lesssim \eta_j, \tag{4.44}$$

uses (4.41), (4.42) and it is equivalent to [5] or to [4, Lemma 4.1] and we omit it for brevity.

On the other hand, to bound $\| u_j - u^c_{j,hp} \|_{\mathrm{E},\mathcal{T}}$ in (4.43), we split $a_{hp,\kappa,s}(\cdot,\cdot) = D_{hp}(\cdot,\cdot) + C_{hp}(\cdot,\cdot)$ where

$$D_{hp}(u,v) = \sum_{K \in \mathcal{T}} \int_K \mathcal{A}(\nabla + i\kappa)u \cdot \overline{(\nabla + i\kappa)v} + su\mathcal{B}\overline{v}\, dx + \sum_{F \in \mathcal{F}(\mathcal{T})} \frac{\gamma p_F^2}{h_F} \int_F [\![u]\!] \cdot \overline{[\![v]\!]}\, ds,$$

$$C_{hp}(u,v) = -\sum_{F \in \mathcal{F}(\mathcal{T})} \int_F \{\!\!\{\mathcal{A}(\nabla + i\kappa)u\}\!\!\} \cdot \overline{[\![v]\!]}\, ds - \sum_{F \in \mathcal{F}(\mathcal{T})} \int_F \{\!\!\{\mathcal{A}\overline{(\nabla + i\kappa)v}\}\!\!\} \cdot [\![u]\!]\, ds.$$

The form $D_{hp}(u,v)$ is well-defined for $u,v \in \mathcal{S}(h)$, whereas $C_{hp}(u,v)$ is only well-defined for discrete functions $u,v \in S_{\underline{p}}(\mathcal{T})$. Furthermore, we have

$$a_{\kappa,s}(u,v) = D_{hp}(u,v) \qquad \forall\, u,v \in H^1_\pi(\Omega), \tag{4.45}$$

as well as

$$a_{hp,\kappa,s}(u,v) = D_{hp}(u,v) + C_{hp}(u,v) \qquad \forall\, u,v \in S_{\underline{p}}(\mathcal{T}). \tag{4.46}$$

Lemma 4.2: For any $v \in H^1_\pi(\Omega)$, we have

$$\int_\Omega \delta_j u_j \mathcal{B}\overline{(v - v_{hp})}\, dx - D_{hp}(u_{j,hp}, v - v_{hp}) + C_{hp}(u_{j,hp}, v_{hp}) \lesssim \left(\eta_j + E_{hp} \right) \| v \|_{\mathrm{E},\mathcal{T}} ,$$

where

$$E_{hp} = \frac{h}{p}\|\lambda_j u_j - \lambda_{j,hp} u_{j,hp}\|_0 + \frac{h}{p}s\|u_j - u_{j,hp}\|_0 .$$

Here, $v_{hp} \in S_{\underline{p}}(\mathcal{T})$ is the hp-approximation of v satisfying (4.40).

Proof. For brevity, let us set

$$T = \int_\Omega \delta_j u_j \mathcal{B}\overline{(v - v_{hp})}\, dx - D_{hp}(u_{j,hp}, v - v_{hp}) + C_{hp}(u_{j,hp}, v_{hp}).$$

Integrating the volume terms by parts we obtain

$$T = \sum_{K \in \mathcal{T}} \int_K (\delta_j u_j \mathcal{B} + (\nabla + i\kappa) \cdot \mathcal{A}(\nabla + i\kappa)u_{j,hp} - su_{j,hp}\mathcal{B})(\overline{v - v_{hp}}) \, dx$$

$$- \sum_{F \in \mathcal{F}(\mathcal{T})} \frac{\gamma p_F^2}{h_F} \int_F [\![u_{j,hp}]\!] \cdot [\![\overline{v - v_{hp}}]\!] \, ds$$

$$- \sum_{F \in \mathcal{F}(\mathcal{T})} \int_F [\![\mathcal{A}(\nabla + i\kappa)u_{j,hp}]\!] \{\!\{\overline{v - v_{hp}}\}\!\} \, ds - \sum_{F \in \mathcal{F}(\mathcal{T})} \int_F \{\!\{\overline{\mathcal{A}(\nabla + i\kappa)v_{hp}}\}\!\} \cdot [\![u_{j,hp}]\!] \, ds$$

$$\equiv T_1 + T_2 + T_3 + T_4.$$

Using the Cauchy-Schwarz inequality and the approximation properties (4.40) and recalling that $\delta_j - s = \lambda_j$ and that $\delta_{j,hp} - s = \lambda_{j,hp}$ we have that

$$T_1 = \sum_{K \in \mathcal{T}} \int_K (\lambda_{j,hp}\mathcal{B}u_{j,hp} + (\nabla + i\kappa) \cdot \mathcal{A}(\nabla + i\kappa)u_{j,hp})(\overline{v - v_{hp}}) \, dx$$

$$+ \sum_{K \in \mathcal{T}} \int_K (\lambda_j u_j - \lambda_{j,hp}u_{j,hp})\mathcal{B}(\overline{v - v_{hp}}) + s(u_j - u_{j,hp})\mathcal{B}\overline{(v - v_{hp})} \, dx$$

$$\lesssim \Big(\sum_{K \in \mathcal{T}} \eta_{j,R_K}^2 \Big)^{\frac{1}{2}} \| v \|_{\mathrm{E},\mathcal{T}} + \frac{h}{p}\|\lambda_j u_j - \lambda_{hp}u_{j,hp}\|_0 \| v \|_{\mathrm{E},\mathcal{T}} + \frac{h}{p}s\|u_j - u_{j,hp}\|_0 \| v \|_{\mathrm{E},\mathcal{T}}.$$

For term T_2, we again exploit the Cauchy-Schwarz inequality to conclude that

$$T_2 \leq \Big(\sum_{F \in \mathcal{F}(\mathcal{T})} \gamma^2 p_F^3 h_F^{-1} \|[\![u_{j,hp}]\!]\|_{0,F}^2 \Big)^{\frac{1}{2}} \Big(\sum_{F \in \mathcal{F}(\mathcal{T})} p_F h_F^{-1} \|[\![\overline{v - v_{hp}}]\!]\|_{0,F}^2 \Big)^{\frac{1}{2}}.$$

Thus, from (3.11), (3.12) and (4.40), we obtain the bound

$$T_2 \lesssim \Big(\sum_{K \in \mathcal{T}} \eta_{j,J_K}^2 \Big)^{\frac{1}{2}} \| v \|_{\mathrm{E},\mathcal{T}}.$$

Similarly, term T_3 can be bounded by

$$T_3 \leq \Big(\sum_{F \in \mathcal{F}_I(\mathcal{T})} p_F^{-1} h_F \|[\![\mathcal{A}(\nabla + i\kappa)u_{j,hp}]\!]\|_{0,F}^2 \Big)^{\frac{1}{2}} \Big(\sum_{F \in \mathcal{F}_I(\mathcal{T})} p_F h_F^{-1} \|\{\!\{\overline{v - v_{hp}}\}\!\}\|_{0,F}^2 \Big)^{\frac{1}{2}}$$

$$\lesssim \Big(\sum_{K \in \mathcal{T}} \eta_{j,F_K}^2 \Big)^{\frac{1}{2}} \| v \|_{\mathrm{E},\mathcal{T}}.$$

In a similar way we use Cauchy-Schwarz inequality, (3.11) and (3.12) also for the term T_4:

$$T_4 \lesssim \gamma^{-1}\Big(\sum_{F\in\mathcal{F}(\mathcal{T})}\gamma^2 p_F^2 h_F^{-1}\|[\![u_{j,hp}]\!]\|_{0,F}^2\Big)^{\frac{1}{2}}\Big(\sum_{K\in\mathcal{T}}p_K^{-2}h_K\|\overline{\mathcal{A}(\nabla+i\kappa)v_{hp}}\|_{0,\partial K}^2\Big)^{\frac{1}{2}}.$$

From the standard hp-version inverse trace inequality, see [7], we conclude that

$$T_4 \lesssim \gamma^{-1}\Big(\sum_{K\in\mathcal{T}}\eta_{j,J_K}^2\Big)^{\frac{1}{2}}\Big(\sum_{K\in\mathcal{T}}\|v_{hp}\|_{1,K}^2\Big)^{\frac{1}{2}},$$

furthermore, using the approximation properties in (4.40),

$$\sum_{K\in\mathcal{T}}\|v_{hp}\|_{1,K}^2 \lesssim \sum_{K\in\mathcal{T}}\|v-v_{hp}\|_{1,K}^2 + \sum_{K\in\mathcal{T}}\|v\|_{1,K}^2 \lesssim \|v\|_{\mathrm{E},\mathcal{T}}^2,$$

where we have assumed safely that $h_K/p_K \lesssim 1$. Hence

$$T_4 \lesssim \gamma^{-1}\Big(\sum_{K\in\mathcal{T}}\eta_{j,J_K}^2\Big)^{\frac{1}{2}}\|v\|_{\mathrm{E},\mathcal{T}}.$$

The bounds for T_1, T_2, T_3, and T_4 imply the assertion. ∎

We are now ready to bound $\|u_j - u_{j,hp}^c\|_{\mathrm{E},\mathcal{T}}$ in (4.43).

Lemma 4.3: Let $(\lambda_{j,hp}, u_{j,hp})$ be a computed eigenpair of (3.24) and let (λ_j, u_j) be an eigenpair of (1.1). Then we have for $u_{j,hp}^c = I_{hp}\,u_{j,hp}$ that:

$$\|u_j - u_{j,hp}^c\|_{\mathrm{E},\mathcal{T}} \lesssim \eta_j + \|\lambda_j u_j - \lambda_{j,hp}u_{j,hp}\|_0 + s\|u_j - u_{j,hp}\|_0.$$

Proof. Since $u_j - u_{j,hp}^c \in H_\pi^1(\Omega)$, we have from [21, Lemma 2.1] that

$$\|u_j - u_{j,hp}^c\|_{\mathrm{E},\mathcal{T}}^2 \lesssim a_{hp,\kappa,s}(u_j - u_{j,hp}^c, v), \qquad (4.47)$$

where $v = u_j - u_{j,hp}^c$. To bound the right-hand side of (4.47), we note that, by (4.45),

$$a_{hp,\kappa,s}(u_j - u_{j,hp}^c, v) = \int_\Omega \delta_j \mathcal{B}u_j\overline{v}\,dx - a_{hp,\kappa,s}(u_{j,hp}^c, v) = \int_\Omega \delta_j \mathcal{B}u_j\overline{v}\,dx - D_{hp}(u_{j,hp}^c, v).$$

It is straightforward to see that $D_{hp}(u_{j,hp}^c, v) = D_{hp}(u_{j,hp}, v) + R$, with

$$R = -\sum_{K\in\mathcal{T}}\int_K \mathcal{A}(\nabla+i\kappa)u_{j,hp}^r\cdot\overline{(\nabla+i\kappa)v}\,dx\ .$$

Furthermore, from (3.30) and (4.46), we have

$$\int_\Omega \delta_{j,hp}\mathcal{B}u_{j,hp}\overline{v_{hp}}\,dx = D_{hp}(u_{j,hp}, v_{hp}) + C_{hp}(u_{j,hp}, v_{hp}),$$

where $v_{hp} \in S_{\underline{p}}(\mathcal{T})$ is the hp-approximation of v. Combining these results, we thus arrive at

$$a_{hp,\kappa,s}(u_j - u_{j,hp}^c, v) = \int_\Omega (\delta_j\mathcal{B}u_j - \delta_{j,hp}\mathcal{B}u_{j,hp})\overline{v_{hp}}\,dx + \int_\Omega \delta_j\mathcal{B}u_j\overline{(v - v_{hp})}\,dx$$

$$-D_{hp}(u_{j,hp}, v - v_{hp}) + C_{hp}(u_{j,hp}, v_{hp}) - R .$$
(4.48)

Using (4.40) we have

$$\|v_{hp}\|_0 \lesssim \|\nabla v\|_0 + \|v\|_0 \lesssim \|v\|_{1,\Omega},$$

then from (4.48) we obtain:

$$a_{hp,\kappa,s}(u_j - u_{j,hp}^c, v) \le \|\delta_j u_j - \delta_{j,hp}u_{j,hp}\|_0 \| v \|_{\mathrm{E},\mathcal{T}} + \int_\Omega \delta_j\mathcal{B}u_j\overline{(v - v_{hp})}\,dx$$

$$-D_{hp}(u_{j,hp}, v - v_{hp}) + C_{hp}(u_{j,hp}, v_{hp}) - R.$$
(4.49)

The estimate from Lemma 4.2 and the fact that

$$\|\delta_j u_j - \delta_{j,hp}u_{j,hp}\|_0 \le \|\lambda_j u_j - \lambda_{j,hp}u_{j,hp}\|_0 + s\|u_j - u_{j,hp}\|_0 ,$$

now yield

$$a_{hp,\kappa}(u_j - u_{j,hp}^c, v) \lesssim \Big(\eta_j + \|\lambda_j u_j - \lambda_{j,hp}u_{j,hp}\|_0 + s\|u_j - u_{j,hp}\|_0\Big)\| v \|_{\mathrm{E},\mathcal{T}} + |R|.$$
(4.50)

It remains to bound $|R|$; from the Cauchy-Schwarz inequality and (4.44), we readily obtain

$$|R| \lesssim \| u_{j,hp}^r \|_{\mathrm{E},\mathcal{T}}\| v \|_{\mathrm{E},\mathcal{T}} \lesssim \eta_j\| v \|_{\mathrm{E},\mathcal{T}}.$$
(4.51)

The desired result now follows from (4.50) and (4.51). $\blacksquare$

The proof of Theorem 4.4 readily follows from (4.43), (4.44) and Lemma 4.3.

Theorem 4.4 (Reliability for eigenfunctions): Let $(\lambda_{j,hp}, u_{j,hp})$ be a computed eigenpair of (3.24) converging to the true eigenvalue λ_j of multiplicity $R+1 > 0$. Then we have that:

$$\mathrm{dist}(u_{j,hp}, E_1(\lambda_j))_{\mathrm{E},\mathcal{T}} \lesssim \eta_j + G ,$$

where

$$G = \|\lambda_j u_j - \lambda_{j,hp}u_{j,hp}\|_0 + s\|u_j - u_{j,hp}\|_0 ,$$

and where u_j is the minimizer of (3.33).

Proof. From (4.43), (4.44) and Lemma 4.3 we have that:

$$\text{dist}(u_{j,hp}, E_1(\lambda_j))_{\text{E},\mathcal{T}} \quad \leq \|u_j - u_{j,hp}^c\|_{\text{E},\mathcal{T}} + \|u_{j,hp}^r\|_{\text{E},\mathcal{T}}$$

$$\lesssim \eta_j + \|\lambda_j u_j - \lambda_{j,hp} u_{j,hp}\|_0 + s\|u_j - u_{j,hp}\|_0 .$$

∎

Theorem 4.5 (Reliability for eigenvalues): Let $(\lambda_{j,hp}, u_{j,hp})$ be a computed eigenpair of (3.30) and converging to λ_j of multiplicity $R + 1 > 0$. Then we have that:

$$|\lambda_j - \lambda_{hp}| \lesssim \eta_j^2 + G' ,$$

where

$$G' = \left(\|\lambda_j u_j - \lambda_{j,hp} u_{j,hp}\|_0 + s\|u_j - u_{j,hp}\|_0\right)^2 + 2\eta_j\left(\|\lambda_j u_j - \lambda_{j,hp} u_{j,hp}\|_0 + s\|u_j - u_{j,hp}\|_0\right)$$

$$+ 2|\mathcal{R}(\hat{u}_j, \hat{u}_j - u_{j,hp})|,$$

where u_j is the minimizer of (3.33) and $\hat{u}_j$ is the minimizer of (3.34).

Proof. Applying (3.32) to Lemma 3.5 and also noticing that $\delta_j\|\hat{u}_j - u_{j,hp}\|_0^2 > 0$ we have

$$|\lambda_j - \lambda_{j,hp}| = |\delta_j - \delta_{j,hp}| \lesssim \text{dist}(u_{j,hp}, E_1(\lambda_j))_{\text{E},\mathcal{T}}^2 + 2|\mathcal{R}(\hat{u}_j, \hat{u}_j - u_{j,hp})| .$$

Applying Theorem 4.4

$$|\lambda_j - \lambda_{j,hp}| \lesssim \left(\eta_j + \|\lambda_j u_j - \lambda_{j,hp} u_{j,hp}\|_0 + s\|u_j - u_{j,hp}\|_0\right)^2 + 2|\mathcal{R}(\hat{u}_j, \hat{u}_j - u_{j,hp})|.$$

∎

Remark 4.6: The terms G and G' are not computed since they are higher order terms [33].

The proof for the efficiency of the error estimator η_j follows standard arguments involving bubble functions ([32, Lemma 3.3]), that have been already presented in [33, 32] and in other papers, so for sake of brevity we are omitting the proofs of the following lemmas. As already mentioned in other paper, i.e. [2, 4], the efficiency result is robust only in h.

Lemma 4.7: Let $(\lambda_{j,hp}, u_{j,hp})$ be a computed eigenpair of (3.24) and converging to λ_j of multiplicity $R + 1 > 0$. Then we have that:

$$\left(\sum_{K \in \mathcal{T}_K} \eta_{j,J_K}^2\right)^{1/2} \lesssim \text{dist}(u_{j,hp}, E_1(\lambda_j))_{\text{E},\mathcal{T}} .$$

Lemma 4.8: Let $(\lambda_{j,hp}, u_{j,hp})$ be a computed eigenpair of (3.24) converging to eigenvalue λ_j of multiplicity $R + 1 > 0$. Then we have that:

$$\Big(\sum_{K \in \mathcal{T}_K} \eta_{j,R_K}^2 \Big)^{1/2} \lesssim \operatorname{dist}(u_{j,hp}, E_1(\lambda_j))_{\mathrm{E},\mathcal{T}} + \frac{h}{p}\|\lambda_{j,hp}u_{j,hp} - \lambda_j u_j\|_0 + \frac{h}{p}s\|u_j - u_{j,hp}\|_0,$$

where u_j be the minimizer of (3.34).

Lemma 4.9: Let $(\lambda_{j,hp}, u_{j,hp})$ be a computed eigenpair of (3.24) and converging to λ_j of multiplicity $R + 1 > 0$. Then we have that:

$$\Big(\sum_{K \in \mathcal{T}_K} \eta_{j,F_K}^2 \Big)^{1/2} \lesssim \operatorname{dist}(u_{j,hp}, E_1(\lambda_j))_{\mathrm{E},\mathcal{T}} + \frac{h}{p}\|\lambda_j u_j - \lambda_{j,hp}u_{j,hp}\|_0 + \frac{h}{p}s\|u_j - u_{j,hp}\|_0,$$

where u_j is the minimizer of (3.34).

The proof of the efficiency result Theorem 4.10 follows in a straightforward manner from Lemmas 4.7-4.9.

Theorem 4.10: Let u_j be an eigenvalue of (2.10) and $u_{j,hp} \in S_{\underline{p}}(\mathcal{T})$ be its DG approximation obtained by (3.24) with γ sufficiently large. Let the error estimator η_j be defined by (4.39). Then we have the bound

$$\eta_j \lesssim \operatorname{dist}(u_{j,hp}, E_1(\lambda_j))_{\mathrm{E},\mathcal{T}} + \frac{h}{p}\|\lambda_{j,hp}u_{j,hp} - \lambda_j u_j\|_0 + \frac{h}{p}s\|u_{j,hp} - u_j\|_0 \ .$$

5   Numerical methods and numerical results

First of all we would like to illustrate with an example and presenting plots and pictures the way to proceed in order to compute the spectrum of a PC. The spectra of photonic crystals typically contain band gaps, but, for many applications, the identification of band gaps is not enough. Commonly it is necessary to create eigenvalues inside the gaps in the spectra of the media. The importance of these eigenvalues is due to the fact that electromagnetic waves, which have frequencies corresponding to these eigenvalues, may remain trapped inside the crystal [17, 19]. The common way to create such eigenvalues is by introducing a localized defect in the periodic structures — see [19] and [18, Theorem 2]. Such localized defects do not change the bands of the essential spectrum [18, Theorem 1]. For sake of brevity we are going to consider only the TE case in this example. In this case $\mathcal{A}$ is piecewise constant, $\mathcal{B} = 1$ and there are typically localized singularities in the gradient of the eigenfunctions at corner points of the interface in the dielectric ε, leading to a strong need for adaptivity.

The first step in order to analyze a PC is to compute the band structure of the periodic structure of the crystal. In this example we consider a square unit cell with a square inclusion of side 0.5 centered inside it. We choose $\mathcal{A}$ to take the value 1 outside the inclusion and the value 0.05 inside it, see Figure 1. This is a realistic example, since expected jumps in dielectric permittivity of real photonic crystals are of this order.
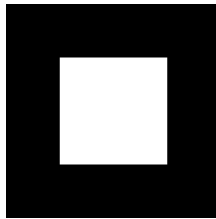

Fig. 1: Structure of the primitive cell.

In order to produce accurately the band structure of the crystal it is just necessary to compute the eigenvalues of (1.1) for the values of κ in the reduced Brillouin zone, see Figure 2, instead of using the entire first Brillouin zone.
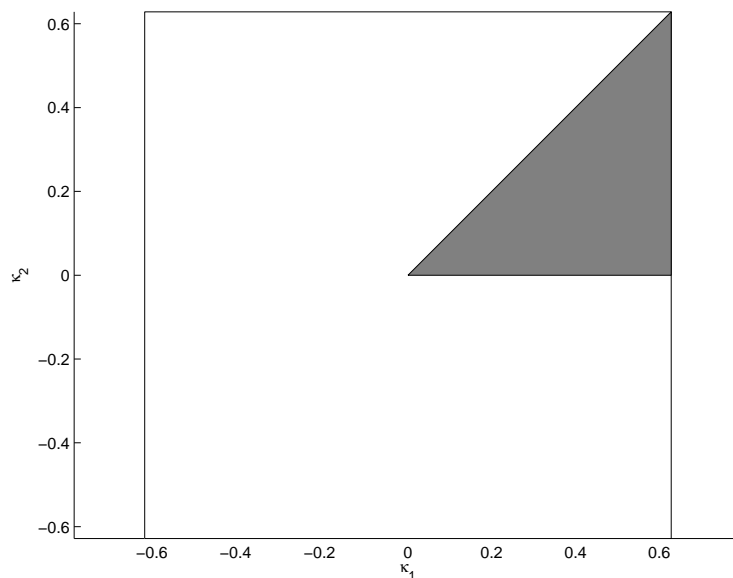
Fig. 2: The dark triangle is the reduced Brillouin zone for the primitive cell in Figure 1.

Each eigenvalue of (1.1) can be seen as a function of the quasimomentum $\lambda_j(\kappa)$, in this way we can obtain the plot in Figure 3, where we have plotted just the first four bands and for sake of clarity we just considered the values of κ on the border of the reduced Brillouin zone. As can be seen the minimum and the maximum of each function $\lambda_j(\kappa)$ delimit a band of the spectrum and between bands sometimes gaps can be found. In this example there is a gap between the first and the second band. The frequencies of light corresponding to points in the gap are not allowed to travel across the periodic structure of the PC.
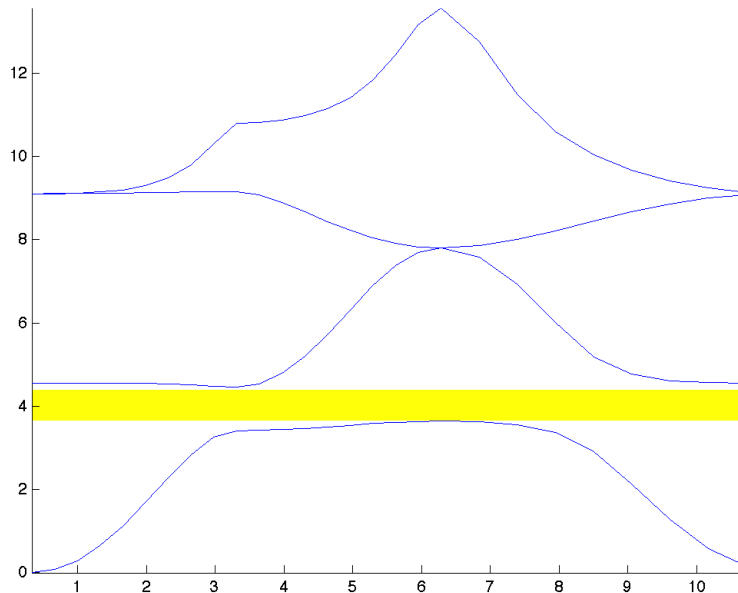
Fig. 3: Band structure of the spectrum for the periodic crystal. The gap between the first two bands has been highlighted in yellow.

Now considering as a primitive cell a bigger portion of the periodic structure, like in Figure 4, has no impact on the presence or positions of gaps in the spectrum, see Figure 5. On the other hand the structure of the bands changed in the way that each band split in a multitude of smaller bands. Now the gap is between the 25th and the 26th band.
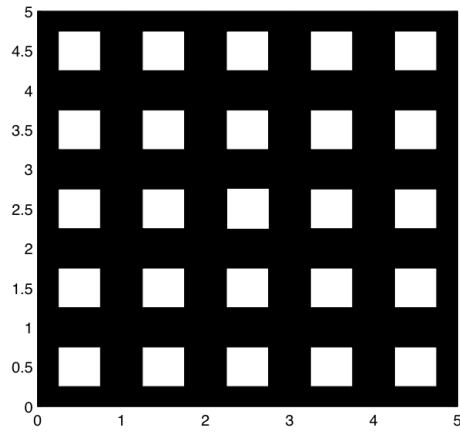
Fig. 4: Structure of the bigger primitive cell.
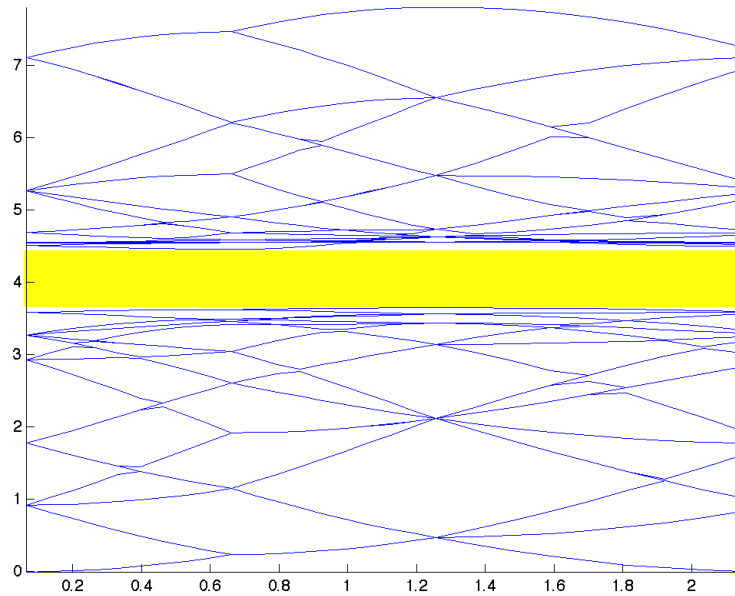
Fig. 5: Band structure of the spectrum for the periodic crystal with primitive cell as in Figure 4. The first gap has been highlighted in yellow.

Finally, as predicted by the theory [23], the presence of a compact defect in the periodic structure can consequently create localized eigenvalues in the gaps that correspond to trapped modes. These modes can travel the

all length of the PC with almost no losses. The best way to search for these trapped mode is to consider the supercell framework [31], in which the considered primitive cell (called supercell) is a portion of the periodic structure including the defect. Since of the periodic boundary conditions, the defect is not any more compact because it is repeated in each supercell, see Figure 6. So the introduction of the defect in the supercell will not lead to the creation of eigenvalues in the gaps but it could create narrow new bands in the gaps which shrink exponentially fast to eigenvalues when the number of layers of periodic structure around the defect in the supercell is increased [21, Table 7]. Computing the band structure of the supercell we obtain Figure 7 where a new narrow band of index $j = 25$ is now present in the first gap.
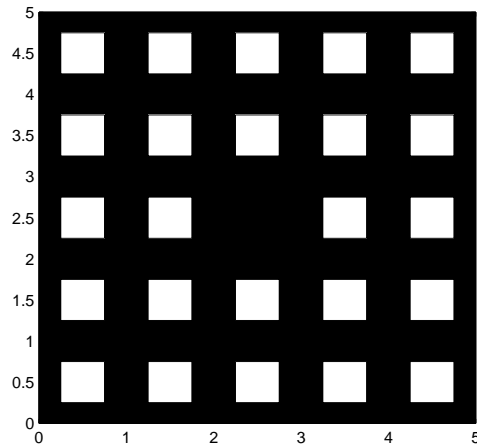
Fig. 6: Structure of the supercell with a defect in the center.
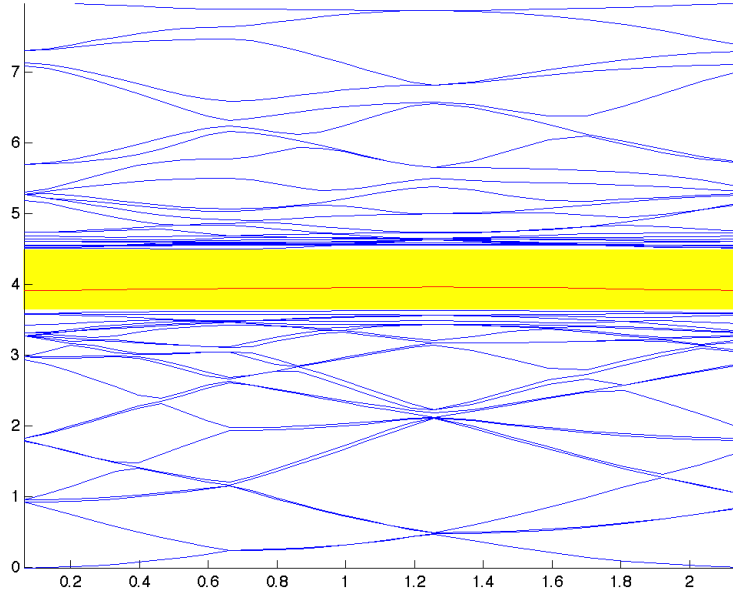
Fig. 7: Band structure of the spectrum for the supecell in Figure 6. The first gap has been highlighted in yellow and the newly created trapped band in red.

So the best way to numerically discover these trapped mode is first to compute the position of the gaps in the spectrum of the periodic structure with no defects and then check for the presence of any band for the supercell problem in span of the already computed gaps for the periodic structure.

This way to proceed, that could seem rather complicated, is numerically efficient because the localization of the gaps is done on the single cell problem, that is a small problem to solve. Then on the supercell with the defect, only the eigenvalues in the gaps are computed. That could be easily done using the shift and invert spectral transformation in ARPACK [24] and setting the shift value to be the middle point of a gap.

The algorithm used to compute all numerical results in this section is presented in Algorithm 1, which takes as input: an initial mesh $\mathcal{T}$, an initial DG space $S_{\underline{p}}$, the index j of the eigenpair to approximate, a real value $0 \leq \theta \leq 1$ to tune the fixed-fraction marking strategy and finally a real and positive value tol which prescribes the required tolerance. The algorithm has a very simple structure that consists of a repeat-until loop. During each iteration of the loop a new approximation of the eigenpair of interest is computed, then the error estimator is calculated and, if the estimated error $\left(\sum_{K \in \mathcal{T}} \eta_{j,K}^2\right)^{1/2}$

is smaller than the prescribed tolerance tol the algorithm stops; otherwise the mesh $\mathcal{T}$ and the space $S_{\underline{p}}$ are refined and another iteration follows. The function Refine applies a simple fixed-fraction strategy to mark a minimal subset of elements containing a portion of the error proportional to θ. Then the choice for each marked element between splitting the element into smaller elements (h-refinement) or increasing the polynomial order (p-refinement) is made by testing the local analyticity of the solution in the interior of the element as described in [36]. In the case that we are only interested to use h-refinement the local analyticity test can be avoided.

Algorithm 1 hp-adaptive algorithm

$(\lambda_{j,hp}, u_{j,hp}) := \text{AdaptDG}(\mathcal{T}, S_{\underline{p}}(\mathcal{T}), j, \theta, \text{tol})$

repeat

    Compute the j-th eigenpair $(\lambda_{j,n}, u_{j,n})$ on $\mathcal{T}$

    Compute $\eta_{j,K}$ for all $K \in \mathcal{T}$

   **if** $\left(\sum_{K \in \mathcal{T}} \eta_{j,K}^2 \right)^{1/2} < \text{tol}$ **then**

      exit

    else

      Refine$(\mathcal{T}, S_{\underline{p}}(\mathcal{T}), \theta, \eta_j)$

    end if

until

5.1   TE case problem on periodic medium

We first consider the TE problem for a periodic medium with primitive cell as in Figure 1 and with the same choice for $\mathcal{A}$ as above.

Starting with a structured mesh of 162 triangular elements and with order of polynomials equal to 2 everywhere, we use Algorithm 1 with either h- or hp-adaptivity. To make the test more complete, we compare the two adaptive strategies for different values of the quasimomentum. Figures (8)-(10) contain the convergence plots for the second eigenvalue for the all considered different values of quasimomentum. It is possible to see that in all cases with the hp-adaptivity the convergence is much faster than with only h-adaptivity. The fact that the curves for the hp-adaptivity approximate a straight line in semi-log scale, suggests a convergence rate close to be exponential. In contrast h-adaptivity delivers only a polynomial rate of convergence, as comes from the theory.
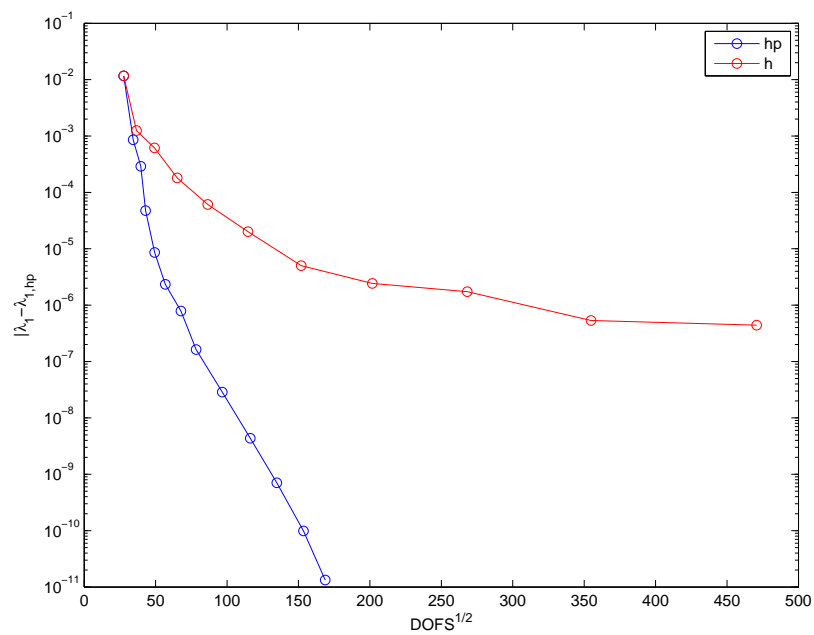
Fig. 8: Convergence plots for quasimomentum $\kappa = (0,0)$
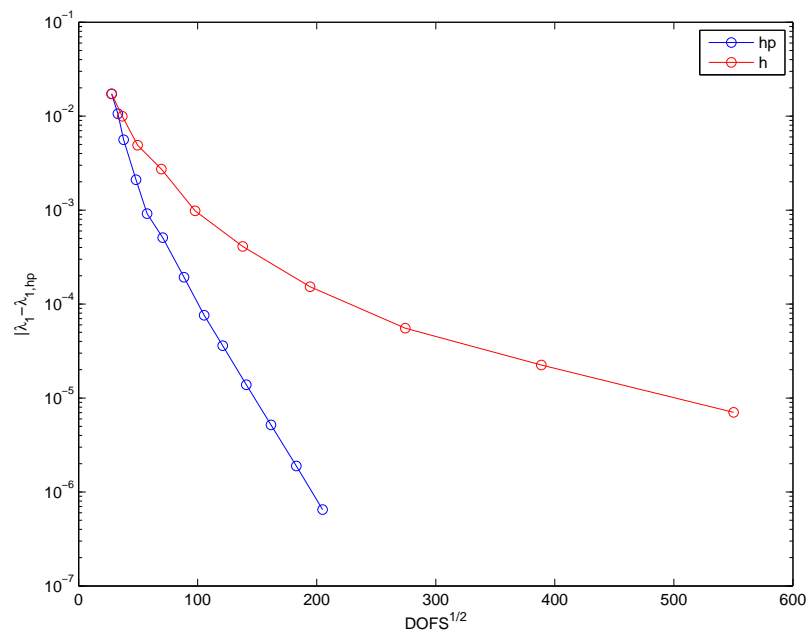
Fig. 9: Convergence plots for quasimomentum $\kappa = (\pi, 0)$
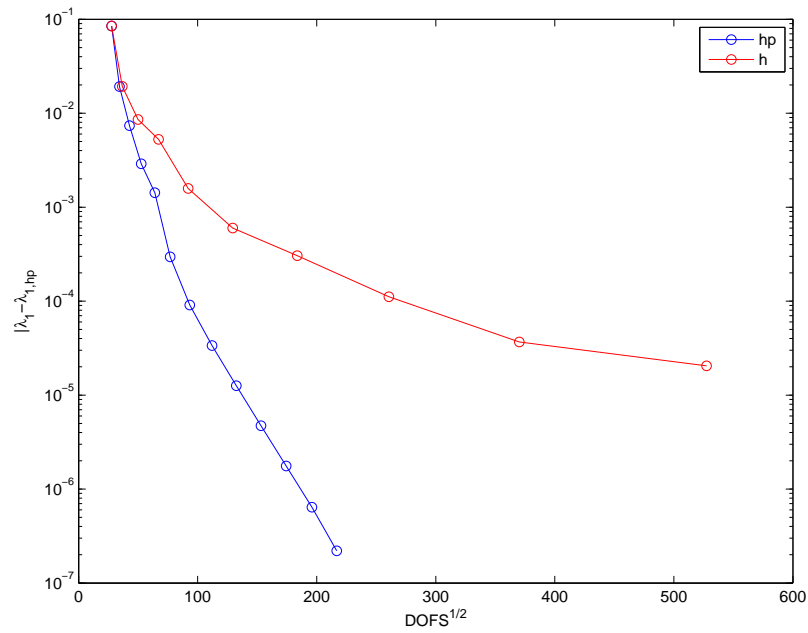
Fig. 10: Convergence plots for quasimomentum $\kappa = (\pi, \pi)$

In Figure 11 we depict the mesh coming from the twelfth iteration of Algorithm 1 using hp-adaptivity. The colors indicate the order of polynomials in each elements, as can be seen in the four corners of the inclusion the elements are very small, sign of possible singularities in the gradient of the eigenfunction. In Figure 12 we depict the eigenfunction corresponding to the eigenvalue in the second band of the problem with quasimomentum $\kappa = (0, 0)$.
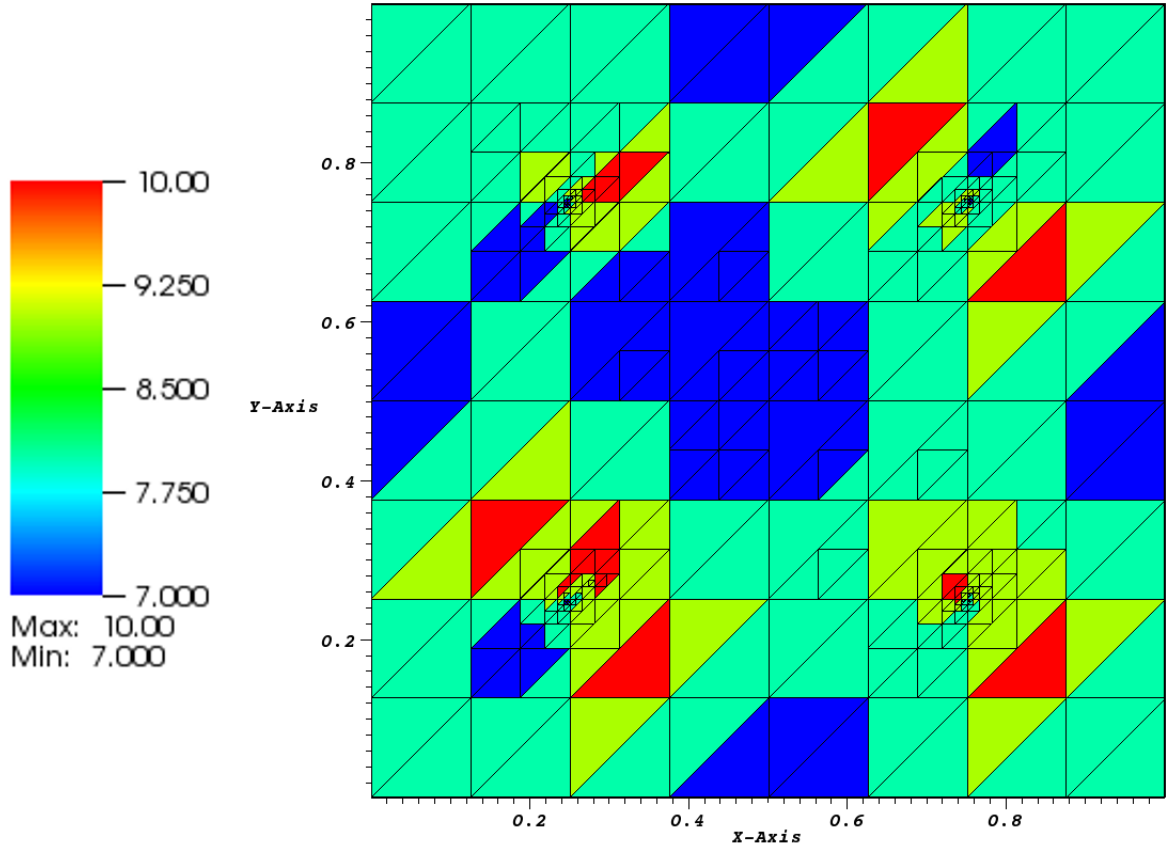
Fig. 11: A refined mesh coming from the hp-adaptive method for $\kappa = (0,0)$.

5.2   TE mode problem on supercell

Now we are interested in approximating the trapped band discovered in Figure 7, in order to do that we are now considering as domain of the problem the supercell in Figure 6. Since now the domain is $[-2.5, 2.5]^2$, it comes that the first Brillouin zone is smaller: $[-\pi/5, \pi/5]^2$. As before we compared h- with hp-adaptivity for different values of the quasimomentum.

Figures (13)-(15) contain the convergence plots for the eigenvalue on the trapped band for the all considered different values of quasimomentum. Again it is possible to see that in all cases with the hp-adaptivity the convergence is much faster than with only h-adaptivity.
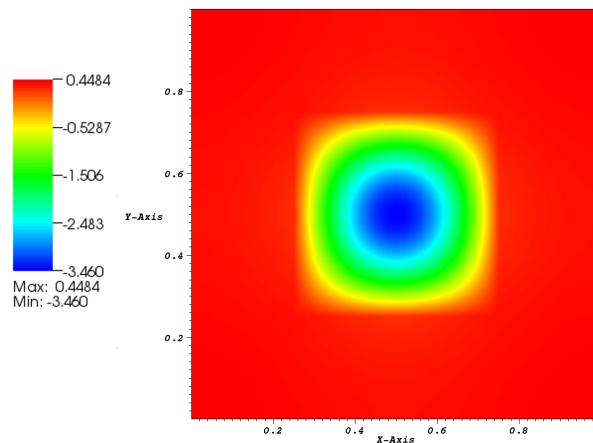
Fig. 12: The eigenfunction of the eigenvalue in the second band of the TE mode problem with quasimomentum $\kappa = (0, 0)$.
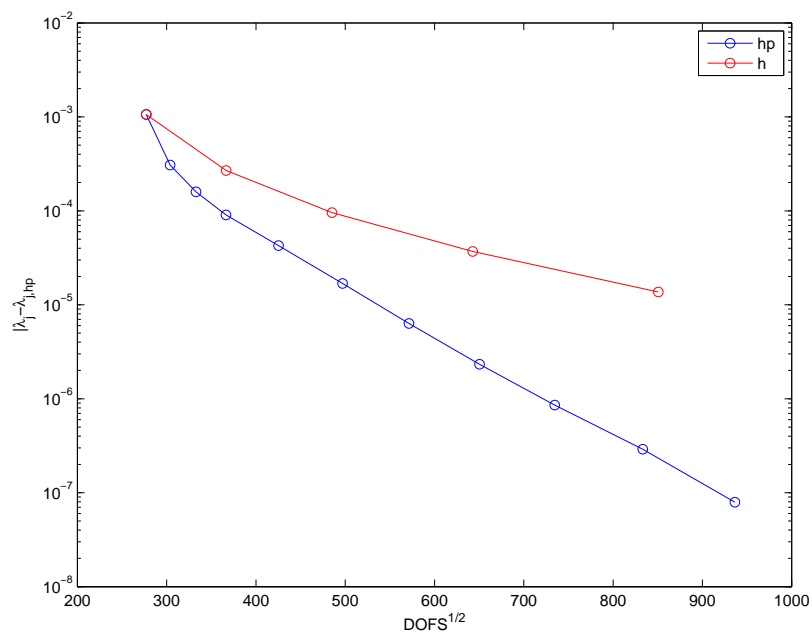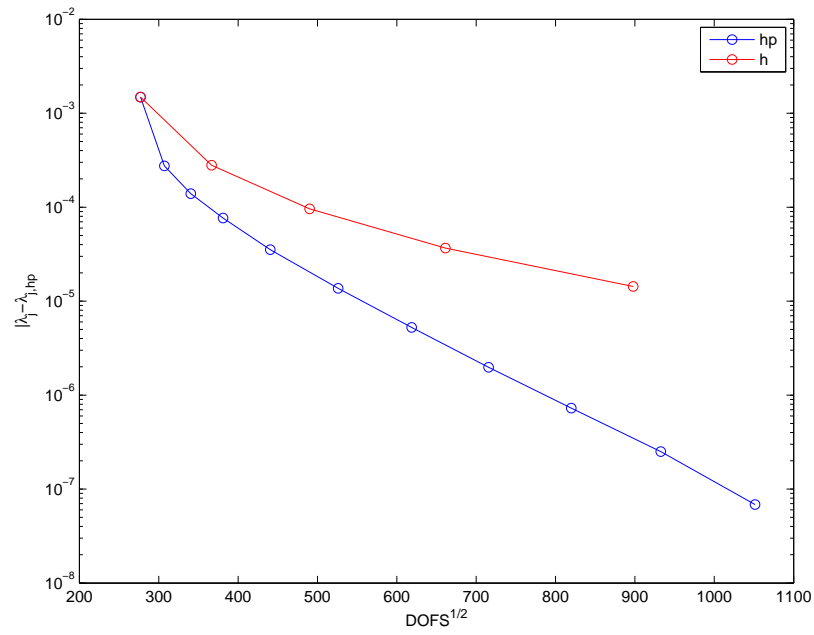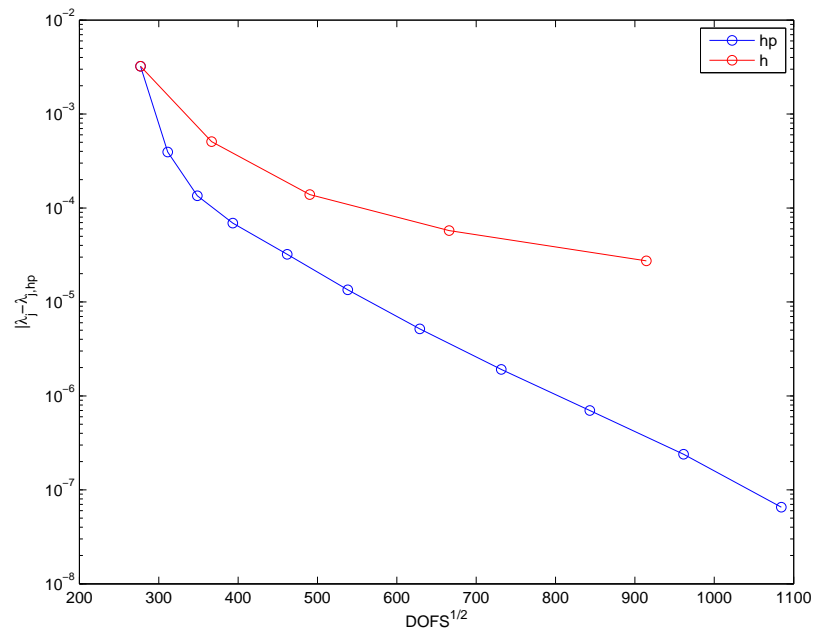

Fig. 13: Convergence plots for quasimomentum $\kappa = (0, 0)$

Fig. 14: Convergence plots for quasimomentum $\kappa = (\pi/5, 0)$

Fig. 15: Convergence plots for quasimomentum $\kappa = (\pi/5, \pi/5)$

In Figure 16 we depict the mesh coming from the fifth iteration of Algorithm 1, as can be seen there is a lot of refinement around the defect,

especially around the corners of the inclusions. Away enough from the defect the corners of the inclusions are not much refined anymore. Since the trapped mode has a fast decay away from the defect, this prevent any strong singularity to appear in the corners of the inclusions far enough from the defect. This is the reason why the refinement is so concentrated near the defect and why the corners of the inclusions away from the defect seem not to show important singularities. In Figure 17 we depict the eigenfunction corresponding to the eigenvalue in the second band of the problem with quasimomentum $\kappa = (0, 0)$.
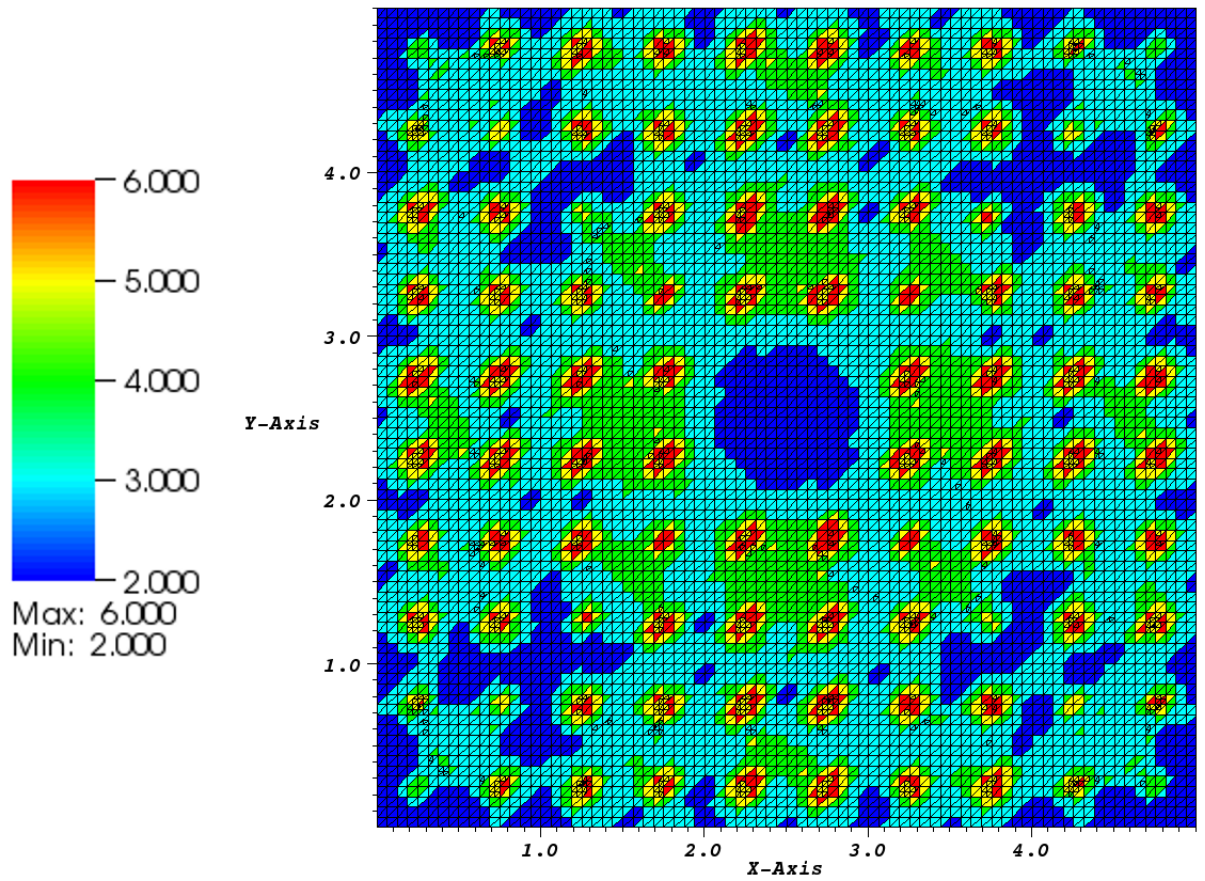
Fig. 16: An adapted mesh for a trapped eigenvalue of the TE case problem
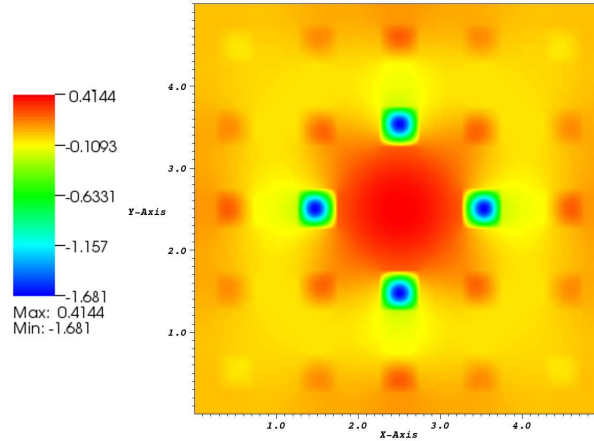   on a supercell with quasimomentum $\kappa = (0, 0)$.

Fig. 17: A picture of the eigenfunction trapped in the defect of the TE case
problem on a supercell with quasimomentum $\kappa = (0, 0)$.

References

[1] D.N. Arnold, F. Brezzi, B. Cockburn and D.L. Marini, Unified Analysis of Discontinuous Galerkin Methods for Elliptic Problems, *SIAM J. Numer. Anal.* 39(5):1749-1779, 2001.

[2] L. Zhu, S. Giani, P. Houston and D. Schoetzau, Energy norm a-posteriori error estimation for hp-adaptive discontinuous Galerkin methods for elliptic problems in three dimensions, *Math. Models Methods Appl. Sci.* 21(2): 267-306, 2011.

[3] P. Houston, E. Süli and T. Wihler, A-posteriori error analysis of *hp*-version discontinuous Galerkin finite-element methods for second-order quasi-linear elliptic PDEs, *IMA J. Numer. Anal.* 28:245-273, 2008.

[4] L. Zhu and D. Schötzau, A robust a-posteriori error estimate for *hp*-adaptive DG methods for convection-diffusion equations *IMA J. Numer. Anal.* , 2010.

[5] P. Houston, D. Schötzau and T. Wihler, Energy norm a-posteriori error estimation of hp-adaptive discontinuous Galerkin methods for elliptic problems. *Comput. Methods Appl. Mech. Engrg.*,194:229-243, 2005.

[6] P. Houston, C. Schwab and E. Süli, Discontinuous hp-finite element methods for advection-diffusion problems, *Technical Report no. 00/15, Oxford University Computing Laboratory, 2000.*

[7] C. Schwab *p-* and *hp-* Finite Element Methods: Theory and Applications to Solid and Fluid Mechanics *Oxford University Press* 1999.

[8] H. Ammari and F. Santosa, Guided waves in a photonic bandgap strucutre with a line defect, *SIAM J. Appl. Math.* 64(6):2018-2033, 2004.

[9] N. W. Ashcroft and N. D. Mermin, *Solid State Physics*, Holt, Rinehart and Winston, Philadelphia, 1976.

[10] W. Axmann and P. Kuchment, An efficient finite element method for computing spectra of photonic and acoustic band-gap materials, *J. Comput. Physics* 150:468-481, 1999.

[11] M.S. Birman and T.A. Suslina, Periodic magnetic Hamiltonian with a variable metric. The problem of absolute continuity, St Petersburg Mth. J. 11: 203-232, 2000.

[12] D. Boffi, M. Conforti and L. Gastaldi, Modified edge finite elements for photonic crystals, *Numer. Math.* 105:249-266, 2006.

[13] Y. Cao, Z. Hou and Y. Liu, Convergence problem of plane-wave expansion method for phononic crystals, *Physics Letters A* 327:247-253, 2004.

[14] D. C. Dobson, An Efficient Method for Band Structure Calculations in 2D Photonic Crystals, *J. Comp. Phys.* 149:363-376, 1999.

[15] D. C. Dobson, J. Gopalakrishnan and J. E. Pasciak, An efficient method for band structure calculations in 3D photonic crystals, *J. Comput. Phys.* 161(2):668-679, 2000.

[16] C. Engström and M. Wang, Complex dispersion relation calculations with the symmetric interior penalty method Int. J. Num. Meth. Engng, 84:849863, 2010.

[17] A. Figotin and V. Gorentsveig, Localized electromagnetic waves in a layered periodic dielectric medium with a defect, *Phys. Rev. B* 58(1):180-188, 1998.

[18] A. Figotin and A. Klein, Localized classical waves created by defects, *J. Stat. Phys.* 86:165-177, 1997.

[19] A. Figotin and A. Klein, Midgap defect modes in dielectric and acoustic media, *SIAM J. Appl. Math.* 58(6):1748-1773, 1998.

[20] S. Giani. *Convergence of Adaptive Finite Element Methods for Elliptic Eigenvalue Problems with Application to Photonic Crystals*, PhD Thesis, University of Bath, 2008.

[21] S. Giani and I. G. Graham, Adaptive finite element methods for computing band gaps in photonic crystals, *Num. Math.*, submitted, 2011.

[22] J. D. Joannopoulos and S. G. Johnson, Block-iterative frequency-domain methods for Maxwell's equations in a planewave basis, *Optics Express* 8:173-190, 2001.

[23] P. Kuchment, *The mathematics of photonic crystals*, SIAM, Frontiers Appl. Math. 22:207-272, 2001.

[24] R. B. Lehoucq, D. C. Sorensen, and C. Yang, ARPACK Users' Guide: Solution of Large-Scale Eigenvalue Problems with Implicitly Restarted Arnoldi Methods, SIAM, 1998.

[25] R. Norton and R. Scheichl, Convergence Analysis of Planewave Expansion Methods for Schroedinger Operators with Discontinuous Periodic Potentials, *SIAM Journal on Numerical Analysis* 47(6):4356-4380 (2010).

[26] R.A. Norton, Numerical Computation of Band Gaps in Photonic Crystal Fibres, Ph.D. thesis, University of Bath, 2008.

[27] G. J. Pearce, T. D. Hedley and D. M. Bird, Adaptive curvilinear coordinates in a plane-wave solution of Maxwell's equations in photonic crystals, *Physical Review B* 71(19):195108, 2005.

[28] K. Sakoda, *Optical Properties of Photonic Crystals*, Springer-Verlag, 2001.

[29] K. Schmidt and P. Kauf, Computation of band structure of two-dimensional photonic crystals with hp finite elements, Comput. Meth. Appl. Mech. Eng. 198: 1249 - 1259, 2009.

[30] K. Schmidt and R. Kappeler, Efficient computation of photonic crystal waveguide modes with dispersive material, Optics Express,18: 7307-7322, 2010.

[31] S. Soussi, Convergence of the supercell method for defect modes calculations in photonic crystals, *SIAM J. Numer. Anal.* 43(3):1175-1201, 2005.

[32] R. Verfürth, *A Review of a Posteriori Error Estimation and Adaptive Mesh Refinement Techniques*, Wiley-Teubner ,1996.

[33] S. Giani and E. Hall, *An a posteriori error estimator for hp-adaptive discontinuous Galerkin methods for elliptic eigenvalue problems Math. Models Methods Appl. Sci.*, submitted, 2011.

[34] A. Ern, A. Stephanses and P. Zunino, A Discontinuous Galerkin method with weighted averages for advection-diffusion equations with locally vanishing and anisotropic diffusivity, *IMA J. Num. Anal.* 29: 235-256, 2009.

[35] E. Süli, C. Schwab and P. Houston hp-DGFEM for Partial Differential Equations with Nonnegative Characteristic Form In B. Cockburn, G. E. Karniadakis, and C. W. Shu, editors, *Discontinuous Galerkin Methods*, volume 11 of *Lectures Notes in Computational Science and Engineering*, pages 221230. Springer, Berlin, 2000.

[36] T. Eibner and J.M. Melenk An adaptive strategy for hp-FEM based on testing for analyticity *Comp. Mech.* 39: 575-595, 2007.